FULL PAPERS
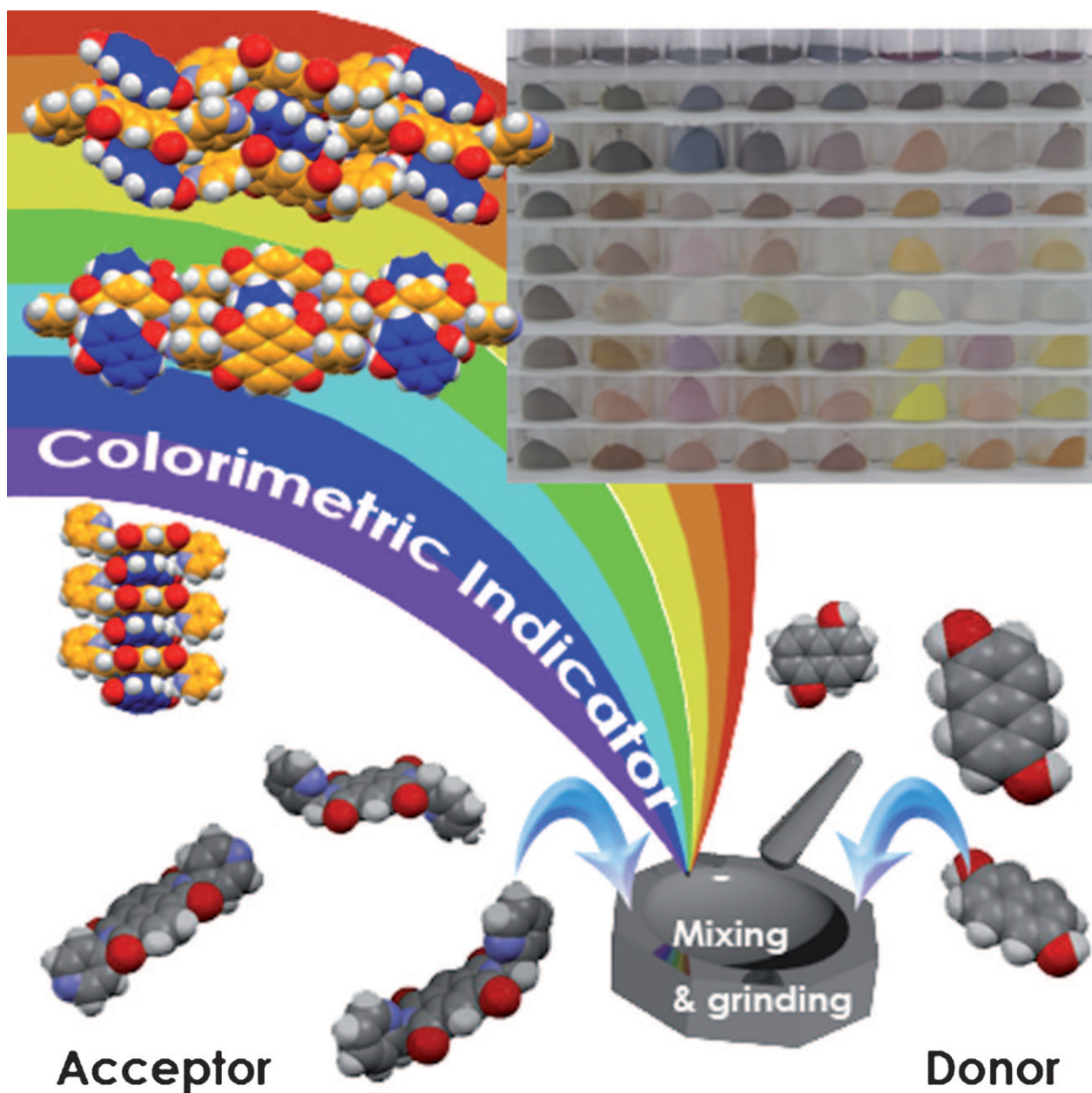
Crystal Engineering Approach To Design Colorimetric Indicator Array To Discriminate Positional Isomers of Aromatic Organic Molecules

Darshak R. Trivedi,[a] Yuzo Fujiki,[a] Norifumi Fujita,[a, b] Seiji Shinkai,[a] and Kazuki Sada*[a]

Abstract: A 2D colorimetric indicator array to discriminate isomers of dihydroxynaphthalene has been designed by using a crystal engineering concept combined with solid-state co-grinding and charge-transfer complexation. The N···H−O supramolecular synthon between the pyridyl N atom of the probe and hydroxy group of the analyte has been observed in all reported single-crystal X-ray structures of resultant CT complexes. Solid-state co-grinding with aromatic solids easily provided the highly concentrated solvent-free conditions required to promote the formation of charge-transfer complexes with brighter color changes. Probe **D** (*N,N′*-bis-(4-pyridyl)pyromellitic diimide) showed an excellent ability to discriminate eight isomers of dihydroxynaphthalene with a wide variety of colors of the resultant CT complexes.

Keywords: charge transfer · crystal engineering · hydrogen bonds · indicators · molecular recognition

Introduction

Colorimetric analysis is the easiest analytical technique for the discrimination of ions and organic molecules, because it can be performed by the naked eye without the need for any analytical tools. Thus, chromogenic phenomena have attracted many supramolecular chemists to develop new functional materials that signal guest recognition by color changes. Most of the colorimetric indicators that have been explored are for the recognition of metal ions[1] and anions,[2] and colorimetric indicators for organic molecules are still in their infancy.[3–5] In particular, it is still not easy to discriminate positional isomers by a simple color change, because their overall electronic structure, and physical and chemical properties are very similar. The design of such a chromogenic device for organic molecules is a challenging task and not yet completely explored in the field of supramolecular chemistry.

Recently, crystal engineering has bloomed as an area of research in supramolecular chemistry and has found potential applications in the design of new functional materials, for example, organogels/hydrogels,[6] ionic liquids,[7] and nonlinear optics.[8]

Our basic design for such colorimetric probes for organic molecules lies in the use of intermolecular charge-transfer (CT) complexes as chromorphores. A pale-colored electron donor acts as an analyte and a pale-colored electron acceptor acts as a probe, or vice-versa. Upon mixing these components, color emerges as a result of the formation of CT complexes with large absorption bands in the visible region. However, in diluted solution, they do not always provoke color changes, because CT complexation is sensitive to mixing conditions, such as solvent polarity and solubility, owing to relatively low formation constants. As a result, it is not easy to use the formation of the intermolecular charge-transfer complexes between aromatic molecules as colorimetric probes. However, this difficulty could be overcome by the solid–solid co-grinding technique.[9] High concentrations of electron donor and electron acceptor in bulk, compared with in solution, enables us to detect the color changes even though they have low formation constants. These results prompted us to investigate the potential of CT complexation as a colorimetric probe for a wide range of aromatic compounds. Herein, we demonstrate a new design of colorimetric probes based on a crystal engineering approach for the determination of aromatic isomers by the naked eye with the aid of solid–solid CT complexation. Our design is based simply on the electron donor or acceptor being chromorphores equipped with binding sites capable of interacting with analytes (Figure 1). Permutations of the electronic structures and stacking modes of the electron-acceptor site of the probe and the electron-donating analytes lead to the formation of strong CT complexes with vivid colors dependent on the analytes.

Thus, we designed acceptor molecules (**A–I**) based on the naphthalene/pyromelletic diimide[10] as colorimetric probes equipped with pyridine rings as binding sites on both arms (Scheme 1), as well as eight geometrical isomers of dihydroxy naphthalene (DHN) as electron-donating analytes. Naphthalene/pyromellitic diimide are well known to be ac-

[a] Dr. D. R. Trivedi, Y. Fujiki, Dr. N. Fujita, Prof. Dr. S. Shinkai, Prof. Dr. K. Sada
Department of Chemistry and Biochemistry
Graduate School of Engineering, Kyushu University
744 Motooka, Nishi, Fukuoka 819-0395 (Japan)
Fax: (+81) 92-802-2820
E-mail: sadatcm@mbox.nc.kyushu-u.ac.jp

[b] Dr. N. Fujita
Present address: Department of Chemistry and Biotechnology
School of Engineering, The University of Tokyo
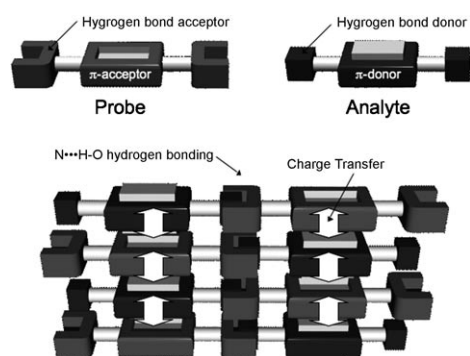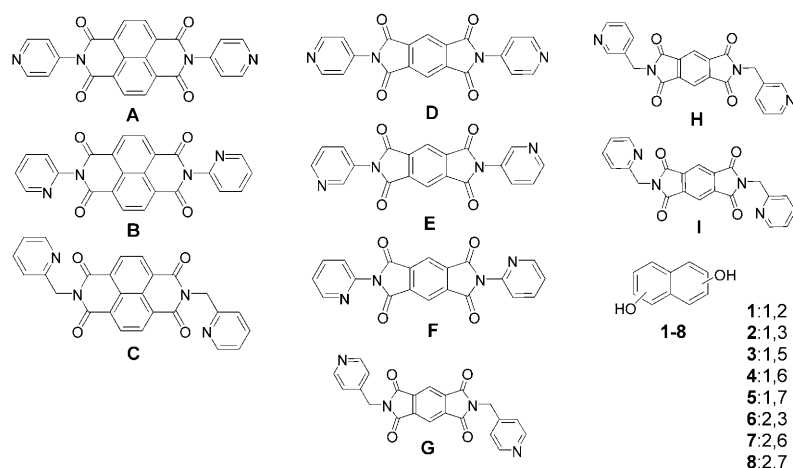7-3-1 Hongo, Bunkyo-ku, Tokyo 113-8656 (Japan)

FULL PAPERS

Figure 1. Design concept of the present study.

Scheme 1. Molecular structures of electron-accepting probes **A–I** and geometrical isomers of dihydroxynaphthalene as electron-donating analytes **1–8**.

ic compounds based on acceptor **A** that did not form one-dimensional columnar structures or π–π stacking structures of naphthalenediimide and various donor groups in the crystalline state.[12] Various electron-accepting probes **A–I** based on naphthalene/pyromellitic diimide were designed as shown in Scheme 1, which represents a 2D colorimetric array. For all the acceptor molecules (**A–I**), we introduced a pyridyl ring at both ends of the diimide backbone because the N atom of the pyridine moieties will take part in intermolecular interactions to enhance the close packing between probe and analyte other than π–π stacking with the hydroxy group of the DHN. The substitution position of the hydroxy group on the naphthalene ring will play a key role, and changes in the direction of the hydroxy group (divergent/convergent) and position of pyridyl N atoms in the probe molecule will facilitate the packing of the acceptor and donor molecules in the crystalline solid state during CT complexation.

It is clear from Figure 2 that the colors of the resultant CT complexes with probes **A** and **B** were not vivid enough to discriminate between the eight isomers of DHN with the naked eye. This result suggests that the position of the pyridyl N atom in the naphthalene diimide based probe molecule does not make a significant difference in the solid-state stacking between the probe and the analyte. In the case of probes **A** and **B**, absorption maxima of the CT complexes were very near to each other, which suggested that probe **A** and **B** did not allow the ability to differentiate between positional isomers of DHN by producing different colors of the CT complexes. The inefficiency of probes **A** and **B** might arise from the rigidity of the probe molecules. In particular, **B**, which has the pyridyl N atom at the 2-position, did not enhance π–π stacking by N···H−O interactions. Probe **C** turned out to be excellent in discriminat-

ceptors, and dihydroxy naphthalenes are donating aromatic species, which easily form CT complexes. Moreover, the introduction of the pyridyl ring into the probes will lead to N···H−O type hydrogen bonds with the phenol hydroxy group of the analytes, which is a well known reliable supramolecular building block in the solid state for arranging functional groups.[11] Furthermore, changing the position of the pyridyl N atom and the introduction of a methylene group as a spacer in the probe will help in modifying the molecular stacking modes or orientating the electron-accepting probes. Herein, we demonstrate combinatorial screening of the vivid color changes in mixtures of electron-accepting probes and electron-donating analytes by solvent-free solid-state co-grinding towards the development of a 2D colorimetric array for the identification of geometrical isomers by simply using the naked eye.
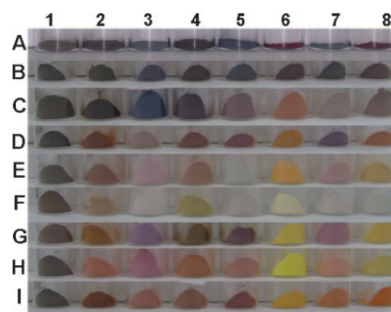
Results and Discussion

Color Changes by Solid–Solid Co-grinding

We recently reported the use of solid-state CT complexation for use as a colorimetric probe to discriminate toxic aromat-

Figure 2. 2D colorimetric indicator array of CT complexes of acceptor molecules **A–I** with eight isomers of DHN (**1–8**).

ing analytes **5–8**, but it had difficulty distinguishing **1–4** because the resultant CT complexes have similar colors (shades of brown). Insertion of a methylene group as a spacer between the diimide and pyridyl ring facilitated CT complexation and resulted in a greater variation of the colors for **C** than for **A** and **B**. For probe **E**, the colors of the CT complexes for **3** and **7**, as well as **2** and **4**, were similar to each other, which makes them unsatisfactory as colorimetric probes in the present study. Pale colors of the CT complexes with probe **F** suggests that the CT interaction was not strong and this may be because of the rigidity of the acceptor molecules as well as the positions of the pyridyl N atoms. Probes **G** to **I** produce bright colors with the analytes. The absorption bands are very near to each other in the visible region, and it is difficult to discriminate between isomeric organic molecules in the present study by using only the naked eye. Probe **D** was able to discriminate the eight isomers of DHN by the vivid colors of the resultant CT complexes. The λ_{max} values of the resultant CT complexes are in different regions of the visible spectrum (Figure S1 in the Supporting Information). Probe **D** forms a CT complex that is slate grayish with **1**, Indian red with **2**, light gray with **3**, chocolate colored with **4**, dark red with **5**, orange with **6**, dark magenta with **7**, and dark orange with **8**. Analytes **6** and **8** formed paler-colored CT complexes with most of the probe molecules than other isomers of DHN with the same probe molecule, which suggests that the highly convergent derivative **6** (2,3-dihydroxynaphthalene) as well as the highly divergent derivative **8** (2,7-dihydroxynaphthalene) could not facilitate close packing of the aromatic plane to form a strong CT complexation. Analytes **3** (1,5-dihydroxynaphthalene) and **5** (1,7-dihydroxynaphthalene) formed CT complexes with higher λ_{max} values with all the probe molecules, which suggests that the direction of the hydroxy group is suitable for close packing in the solid state.

Single Crystal X-ray Analysis

As discussed earlier, colorimetric probes to discriminate isomeric organic molecules were designed by using a crystal engineering approach based on guest recognition by a supramolecular N···H−O type synthon.[11] It was worthwhile to study single crystals of the resultant CT complexes to get detailed information about the role of the substitution position of the hydroxy group in the analytes and the positions of the pyridyl N atoms in the probes. Although the low binding constant of the CT complexes in the solution state was the main hindrance for obtaining many single crystals of the resultant CT complexes from the 2D colorimetric array, single-crystal X-ray analyses were performed for **A3**, **A7**, **G7**, **I3**, and **I7**.

In all single-crystal X-ray analyses, 1:1 molecular adducts between the probe and the analyte were found. **A3**, **I3**, and **I7** crystallized in triclinic space groups, whereas **A7** and **G7** crystallized in monoclinic space groups. In each case, intermolecular π–π stacking interactions were observed between the diimide unit of the probes and the aromatic analytes, and other secondary weak interactions (e.g., C−H···O, C−H···π) were observed which led to close packing of the probe and the analyte in the solid state.

N···H−O Supramolecular Synthon

In the packing diagrams of all crystal structures, N···H−O type hydrogen bonds were observed between the pyridyl N atom of the probe and hydroxy groups of the analytes. However there was a difference in the overall hydrogen-bonded networks because of the different directions and substitution positions in the probe and the analyte.

Figure 3a shows various types of the hydrogen-bonded networks constructed by the N···H−O synthon in the solid state. In **A3** and **A7**, the probe and analyte were self-assem-
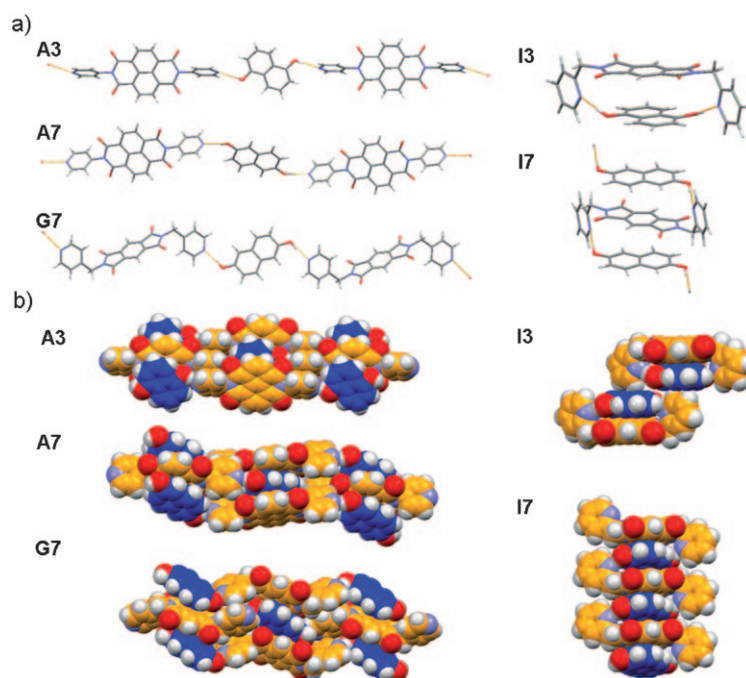

Figure 3. a) N···H-O type synthon observed in all five single crystals studied herein: a linear tape type hydrogen-bonded network is observed in **A3** and **A7**, a cyclic 0D hydrogen-bonded network is observed in **I3**, an infinite zigzag network is observed for **G7**, and a 1D columnar hydrogen-bonded network is observed for **I7**; b) packing diagrams (space-filling model) of the **A3**, **A7**, **G7**, **I3**, and **I7** CT complexes; the probe molecules are shown in orange and the analytes in blue. In all cases, oxygen and nitrogen atoms are shown in red and blue, respectively.

bled by N···H−O type hydrogen bonds, which propagate along the crystallographic *c* axis and form infinite 1D linear tapes of the N···H−O synthon. An infinite zigzag chain type motif was observed for the N···H−O hydrogen bonds in the **G7** CT complex. **I3** self-assembled as a discrete 0D hydrogen-bonded network with the N···H−O synthon. The 0D network is constructed because the probe molecule acted as a "cleft" type host owing to the convergent substituent groups, both of the hydroxy groups of the analyte were hydrogen-bonded to the two pyridyl N atoms of the same probe molecule. This 1D to 0D alteration was governed by the conformation of the probe molecule. Figure 3a shows that in the case of **A3**, **A7**, **G7**, and **I7** the pyridyl rings are on opposite (*anti*) sides of the central diimide moiety, whereas they are on the same side (*syn*) in **I3**. This linear 1D network was transformed into a columnar network in probe **I** with analyte **7** because the 2-pyridyl pyromellitic derivative probe molecule and hydrogen-bonded network run along the CT complexation column.

π–π Stacking and Other Weak Interactions

Figure 3b shows a packing diagram of the π–π stacking interactions in all five X-ray crystal structures. Offset packing of the aromatic plane of the probe and the analyte resulted in strong π–π stacking interactions. The centroid distances between two aromatic moieties were found to be 3.880 and 3.476 Å for **A3** and **A7**, respectively. The analytes adopted different orientations based on the direction of the hydroxy groups to sustain the N···H−O hydrogen bond. The tilted orientations of the analyte facilitated secondary C−H···O interactions within the two probe molecules and led to a closer packing between probe and analyte in **A7** than in **A3**, in which only two carbonyl O atoms (C=O) are involved in C−H···O interactions to form 0D dimer motifs of the probe molecules.

Offset packing of two aromatic rings of the probe and the analyte resulted in strong CT complexation in **G7**. The centroid distance between two π planes is 4.240 Å in the **G7** CT complex. A discrete 1:1 complex was observed for CT complex **I3**, in which strong π–π stacking interactions between the probe and the analyte are further enhanced by N···H−O hydrogen bonds. This 0D complex was extended into a 1D columnar network by edge-to-face type C−H···π interactions between a pyridyl H atom and the aromatic plane of the analyte in **I3**. Two pairs of probe and analyte in the **I7** CT complex form a 1D columnar network by π–π stacking, which is further supported by N···H−O hydrogen bonds in the same direction.

Orientation of the Pyridyl Ring

The two pyridyl arms in probes **C** and **G–I** can rotate freely around the methylene group to allow a variety of conformations. Theoretically, the probe can take on any one of four possible conformations, which means that the two pyridyl rings can be located on either the same or opposite sides of the central diimide moiety, and the N atoms of the pyridyl rings can point in either the same or opposite directions. However, the results were quite surprising. In the case of **G7** and **I7**, the pyridyl rings in the probe molecules were located on opposite sides of core diimide moiety, whereas the pyridyl rings of the probe molecule were located on the same side of the central diimide backbone in the **I3** CT complex.

Close examination of Table 1 and Figure 3b reveals that the centroid distance between aromatic rings (π–π stacking) in the solid state is directly correlated to the absorption maximum of the resultant CT complexes. In the case of probe **A**, the distance between two π planes is shorter in **A7** than in **A3**, which corresponds to a higher value of λ_{max} in the visible region for **A7**. For probe **I**, the centroid distance is shorter in **I3** than in **I7**, and the value of λ_{max} is also higher for **I3**. It is clear from the above crystallographic analysis that both the substituent position of DHN and the positions of pyridyl N atoms play a key role in the overall close packing of the CT complexes in the solid state. Thus, it is possible to tune the π–π stacking between two aromatic planes incorporating other weak nonbonded interactions by using a crystal engineering approach.

Table 1. Typical distances, angles, and λ_{max} values of the CT complexes studied herein.

	A3	A7	G7	I3	I7
O···N distance [Å]	2.751	2.802	2.744	2.773 2.755	2.776
∡O−H···N [°]	170.1	164.8	167.2	173.0 175.0	169.0
dihedral angle between middle diimide and pyridyl ring in the probe [°]	59.98	62.92	72.61	87.48 88.06	86.78
distance between two π planes (probe and analyte centroids) [Å]	3.880	3.476	4.240	3.294	3.444
λ_{max} [nm]	573	604	516	498	475

The dihedral angle between the pyridyl ring and middle diimide moiety was found to be an important parameter for the close packing of probe and analyte in the solid state. The dihedral angle (*θ*) is defined as the angle between two planes passing through the pyridyl ring and the middle diimide moieties, as shown in Figure S2 of the Supporting Information. For probe **A**, there is no methylene spacer between the middle diimide and the pyridyl rings, resulting in a rigid arrangement of the pyridyl rings. The pyridyl rings in **A3** and **A7** form symmetrical dihedral angles of 59.98 and 62.92°, respectively. These values are lower than that of the neat probe molecule with DMF solvate (69.5°; Refcode: GATXAB).[13] Probe **G** is equipped with a methylene spacer and forms a symmetrical dihedral angle of 72.61° in the case

of **G7**. Probe **I** forms unsymmetrical dihedral angles in the case of **I3** of 87.48 and 88.06° and a symmetrical angle in **I7** of 86.78°. The positions of the pyridyl N atoms in the probe molecules play a key role in the orientation of probe molecules in the CT complexes, as the value of the dihedral angle is higher for probe **I** (2-pyridyl) than for **G** (4-pyridyl) because of the strong N···H−O hydrogen bonding between the probe and the analyte. It is clear from Table 1 that a higher dihedral angle is preferred for close packing of probe and analyte in the crystalline state to sustain N···H−O type interactions and for strong CT complexation. Table 1 shows that in all cases, a larger dihedral angle results in a higher value of λ_{max} for the resultant CT complexes.

In all single-crystal X-ray structures, the hydroxy groups of the analyte arranged in such a way to form N···H−O hydrogen bonds with the pyridyl N atoms of the probe, and hence, differences in the orientation were observed in the resultant CT complexes (Figure 4). In the **A3**, **A7**, and **G7** CT complexes, π–π stacking runs perpendicular to the N···H−O interaction, because the pyridyl N atom of the probe molecule is in the 4-position, whereas in the case of the **I3** and **I7** CT complexes, the π–π stacking and N···H−O interactions are in same direction because of the orientation of the pyridyl N atom at the 2-position in the probe.
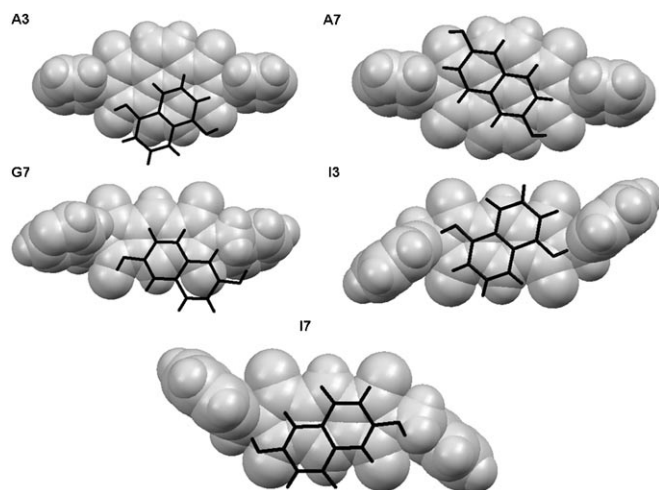

Figure 4. Overlaps and orientations of the probe and the analyte in the **A3**, **A7**, **G7**, **I3**, and **I7** CT complexes; analyte molecules are shown in black (capped sticks model) and probe molecules are shown in gray (space-filling model).

X-ray powder diffraction patterns (XRPD) simulated from the single-crystal data were compared with those obtained from the bulk solid synthesized by solid-state co-grinding of reported CT complexes to establish the molecular packing in the bulk solid and in the corresponding single crystals obtained from solution (Figure S3 of the Supporting Information). Figure S3 of the Supporting Information reveals that in the case of **A7**, **G7**, **I3**, and **I7** the corresponding major peak positions match those in the simulated patterns and XRPD of the bulk solids. Therefore, it may be

concluded that the respective patterns in these CT complexes were nearly identical, which indicates that the molecular packing of the CT complexes obtained from single-crystal X-ray diffraction truly represents the molecular packing in the bulk solids synthesized by solid-state co-grinding. However, the simulated XRPD pattern is quite different from the XRPD of the bulk solid in the case of the **A3** CT complex, which suggests that the single crystal obtained from solution is a different polymorph of resultant CT complex.

Conclusions

In summary, we designed a series of acceptor molecules as probes to prepare a 2D colorimetric indicator array to discriminate between isomers of organic molecules using the naked eye. We used a crystal engineering approach combined with charge-transfer complexation and solid-state co-grinding. Probe **D** showed a wide variety of colors induced by the analyte molecules to allow discrimination of eight isomers of DHN by the vivid color changes. X-ray crystallography studies revealed that all the CT complexes had both N···H−O interactions between hydroxy groups of the analyte and the pyridyl N atoms of the probe as well as CT complexation between the donors and acceptors. The vivid colors originated from perturbation of the CT complexation and varied according to the distance between the two π clouds in the solid state. The positions of the hydroxy groups of the analyte play a key role for the molecular packing in the solid state, and thus fine tuning of the colors is possible by the crystal engineering approach. However, it is still difficult to predict the packing patterns of the probe and the analyte in the solid state by present hypotheses, which opens new challenges for crystal engineering researchers. The highly convergent derivative **6** (2,3-dihydroxynaphthalene) and highly divergent derivative **8** (2,7-dihydroxynaphthalene) could not facilitate close packing in the solid state, whereas analytes **3** (1,5-dihydroxynaphthalene) and **5** (1,7-dihydroxynaphthalene) formed CT complexes with higher λ_{max} values with all the probe molecules, which suggests that the direction of the hydroxy group is suitable for close packing in the solid state. Herein, we have derived the governing parameters for the close packing of two π clouds that lead to CT complexation and correlated this to the absorption maxima of the resultant CT complexes. Thus, crystal engineering should be a powerful tool for the development of future indicator devices. We believe that such a design concept could play a significant role in the development of a new generation of colorimetric indicators or reagents for the identification of target organic guest by solid–solid co-grinding.

Table 2. Crystallographic parameters for the **A3**, **A7**, **G7**, **I3**, and **I7** CT complexes.

	A3	A7	G7	I3	I7
formula	$C_{17}H_{10}N_2O_3$	$C_{17}H_9N_2O_3$	$C_{16}H_{11}N_2O_3$	$C_{32}H_{22}N_4O_6$	$C_{16}H_{11}N_2O_3$
formula weight	290.27	289.26	279.27	558.54	279.27
T [K]	293(2)	293(2)	293(2)	293(2)	293(2)
crystal system	triclinic	monoclinic	monoclinic	triclinic	triclinic
space group	$P\bar{1}$	$P21/c$	$P21/c$	$P\bar{1}$	$P\bar{1}$
crystal size [mm^3]	$0.69 \times 0.65 \times 0.42$	$0.4 \times 0.3 \times 0.09$	$0.62 \times 0.27 \times 0.1$	$0.81 \times 0.17 \times 0.04$	$0.53 \times 0.11 \times 0.03$
crystal color/habit	blue/block	bluish green/fiber	red/fiber	red/thin fiber	orange-yellow/thin fiber
θ range [°]	0.994–22.50	1.83–22.49	1.59–22.50	0.995–25.00	0.996–22.48
a [Å]	7.7593(6)	8.2854(11)	8.4800(15)	7.6259(13)	6.8875(18)
b [Å]	9.1374(7)	6.9513(9)	5.7399(10)	13.045(2)	7.580(2)
c [Å]	9.8283(8)	22.443(3)	26.365(4)	14.088(2)	12.711(3)
α [°]	85.871(2)	90.00	90.00	69.647(3)	95.575(6)
β [°]	80.394(2)	97.046(3)	104.183(6)	76.732(4)	101.443(6)
γ [°]	70.766(2)	90.00	90.00	84.100(4)	96.448(6)
V [Å^3]	648.60(9)	1282.8(3)	1244.2(4)	1278.6(4)	641.4(3)
Z	2	4	4	2	2
ρ_{calcd} [Mg m^{-3}]	1.486	1.498	1.491	1.451	1.446
μ [mm^{-1}]	0.104	0.105	0.105	0.102	0.102
$F(000)$	300	596	580	580	290
reflns collected	1690	1675	1617	4478	1672
independent reflns	1559	1333	1157	2861	1275
R (all data)	0.0543	0.0942	0.0918	0.0956	0.0744
wR (all data)	0.1462	0.2379	0.1443	0.1650	0.1727
GOF on F^2	1.080	1.043	1.056	1.046	1.047
final R	0.0518	0.0799	0.0619	0.0574	0.0599
final wR^2	0.1427	0.2235	0.1336	0.1491	0.1594

Experimental Section

All chemicals of reagent grade were commercially available and used without further purification. ^{1}H NMR spectra were recorded on a Bruker DRX 600 instrument. UV/Vis spectra were recorded on JASCO V-670 spectrophotometer. Elemental analyses were performed on a CHNCORDER MT-5 instrument. XRPD patterns were recorded on a REGAKU R-AXIS instrument.

Syntheses of probes A–I

The corresponding diimide probe molecules were prepared by condensation of naphthalene tetracarboxylic dianhydride or pyromellitic dianhydride (40 mmol) and the corresponding amines (80 mmol) in dehydrated DMF (80 mL). The reaction mixture was heated for 6–8 h at 180 °C. Solid product separated on cooling and was collected by filtration. The compounds were purified by repeated recrystallization from DMF to give the pure compounds in reasonably good yields.

N,N'-Bis-(4-pyridyl)napthalene diimide (A): Elemental analysis (%) calcd for $C_{24}H_{12}N_4O_4$: C 68.57, H 2.88, N 13.33; found: C 67.27, H 3.50, N 12.17. ^{1}H NMR (600 MHz, TFA-d, TMS): $\delta = 8.66$–8.67 (d, 4 H), 9.36 (s, 4 H), 9.44–9.45 ppm (d, 4 H).

N,N'-Bis-(2-pyridyl)napthalene diimide (B): Elemental analysis (%) calcd for $C_{24}H_{12}N_4O_4$: C 68.57, H 2.88, N 13.33; found: C 68.54, H 2.83, N 13.36. ^{1}H NMR (600 MHz, [D$_6$]DMSO, TMS): $\delta = 8.76$ (s, 4 H), 8.69–8.70 (t, 2 H), 8.09–8.12 (m, 2 H), 7.66–7.67 (d, 2 H), 7.59–7.61 ppm (m, 2 H).

N,N'-Bis-(2-pyridylmethyl)napthalene diimide (C): Elemental analysis (%) calcd for $C_{26}H_{16}N_4O_4$: C 69.64, H 3.60, N 12.49; found: C 69.58, H 3.54, N 12.63. ^{1}H NMR (600 MHz, TFA-d, TMS): $\delta = 9.24$ (s, 4 H), 9.12–9.13 (d, 2 H), 8.96–8.99 (t, 2 H), 8.69–8.70 (d, 2 H), 8.34–8.36 (t, 2 H), 6.10 ppm (s, 4 H).

N,N'-Bis-(4-pyridyl)pyromellitic diimide (D): Elemental analysis (%) calcd for $C_{20}H_{10}N_4O_4$: C 64.87, H 2.72, N 15.13; found: C 64.23, H 3.06, N 14.87. ^{1}H NMR (600 MHz, TFA-d, TMS): $\delta = 8.99$–9.00 (d, 4 H), 8.89–8.90(d, 4 H), 8.82 ppm (s, 2 H).

N,N'-Bis-(3-pyridyl)pyromellitic diimide (E): Elemental analysis (%) calcd for $C_{20}H_{10}N_4O_4$: C 64.87, H 2.72, N 15.13; found: C 64.82, H 2.67, N 15.19. ^{1}H NMR (600 MHz, TFA-d, TMS): $\delta = 9.81$ (s, 2 H), 9.47–9.48(d, 2 H), 9.23–9.24 (d, 2 H), 9.04 (s, 2 H), 8.61–8.63 ppm (t, 2 H).

N,N'-Bis-(2-pyridyl)pyromellitic diimide (F): Elemental analysis (%) calcd for $C_{20}H_{10}N_4O_4$: C 64.87, H 2.72, N 15.13; found: C 64.70, H 2.73, N 15.26. ^{1}H NMR (600 MHz, TFA-d, TMS): $\delta = 9.24$–9.26 (d, 2 H), 9.16–9.17(d, 2 H), 9.11–9.13 (d, 4 H), 8.32–8.34 ppm (t, 2 H).

N,N'-Bis-(4-pyridylmethyl)pyromellitic diimide (G): Elemental analysis (%) calcd for $C_{22}H_{14}N_4O_4$: C 66.33, H 3.54, N 14.06; found: C 65.90, H 3.90, N 13.56. 1H NMR (600 MHz, [D$_6$]DMSO, TMS): $\delta = 8.52$–8.53(d, 4 H), 8.37(s, 2 H), 7.36–7.37 (d, 4 H), 4.88 ppm (s, 4 H).

N,N'-Bis-(3-pyridylmethyl)pyromellitic diimide (H): Elemental analysis (%) calcd for $C_{22}H_{14}N_4O_4$: C 66.33, H 3.54, N 14.06; found: C 66.30, H 3.44, N 14.19. ^{1}H NMR (600 MHz, [D$_6$]DMSO, TMS): $\delta = 8.61$(d, 2 H), 8.49–8.50 (d, 2 H), 8.25 (s, 2 H), 7.76–7.78 (d, 2 H), 7.36–7.38 (m, 2 H), 4.87 ppm (s, 4 H).

N,N'-Bis-(2-pyridylmethyl)pyromellitic diimide (I): Elemental analysis (%) calcd for $C_{22}H_{14}N_4O_4$: C 66.33, H 3.54, N 14.06; found: C 65.72, H 3.63, N 13.99. ^{1}H NMR (600 MHz, [D$_6$]DMSO, TMS): $\delta = 8.43$–8.44(d, 2 H), 8.31(s, 2 H), 7.78–7.81 (m, 2 H), 7.42–7.48 (d, 2 H), 7.28–7.30 (m, 2 H), 4.99 ppm (s, 4 H).

Solid-State Co-grinding

In all cases, an equimolar ratio of the probe and analyte were ground in molten pastes. Within 1 min, color changes originating from CT complexation were observed. Prolonged grinding for 10–15 min made the mixture much brighter.

Single-Crystal X-ray Diffraction

In a typical experimental procedure, probe compound (0.1 mmol) was dissolved in hot DMF/toluene mixture (15 mL, 3–5 mL), and a solution of analyte molecule (0.1 mmol) in methanol (10 mL) was layered over it. The solution was allowed to crystallize at room temperature by slow evaporation. Crystals were collected after a few days and used for single-crystal X-ray analysis. Diffraction data were collected at room temperature with Mo$_{K\alpha}$ radiation ($\lambda = 0.7107$ Å) by using a Bruker AXS SMART APEX charge-coupled device diffractometer equipped with a graphite monochromator. The SMART software was used for data collection and

also for indexing the reflections and determining the unit-cell parameters; the collected data were integrated by using SAINT software. The structures were solved by direct methods and refined by full-matrix least-squares calculations with SHELXTL software. All the non-hydrogen atoms were refined anisotropically. The hydrogen atoms were placed at their calculated positions and refined with isotropic displacement coefficients for **A3**, **A7**, and **G7**, and located in the difference Fourier maps for **I3** and **I7**. The crystallographic parameters are listed in Table 2. CCDC 681194 (**A3**), 681195 (**A7**), 681197 (**G7**), 681198 (**I3**), and 681200 (**I7**) contain the supplementary crystallographic data for this paper. These data can be obtained free of charge from The Cambridge Crystallographic Data Centre at www.ccdc.cam.ac.uk/data_request/cif.

Acknowledgements

[1] For copper-responsive fluorescent sensors, see: a) Q. Wu, E. V. Anslyn, *J. Am. Chem. Soc.* **2004**, *126*, 14682; b) M. Royzen, Z. Dai, J. W. Canary, *J. Am. Chem. Soc.* **2005**, *127*, 1612; for lead-specified probes, see: c) T. Hayashita, D. Qing, M. Minagawa, J. C. Lee, C. H. Ku, N. Teramae, *Chem. Commun.* **2003**, 2160; for zinc-selective indicators, see: d) K. Komatsu, K. Kikuchi, H. Kojima, Y. Urano, T. Nagano, *J. Am. Chem. Soc.* **2005**, *127*, 10197; for mercury chemosensors, see: e) M. Matsushita, M. M. Meijler, P. Wirsching, R. A. Lerner, K. D. Janda, *Org. Lett.* **2005**, *7*, 4943; for iron-responsive probes, see: f) Y. Xiang, A. Tong, *Org. Lett.* **2006**, *8*, 1549.

[2] a) L. S. Evans, P. A. Gale, M. E. Light, R. Quesada, *Chem. Commun.* **2006**, 965; b) T. Gunnlaugsson, P. E. Kruger, P. Jensen, J. Tierney, H. D. Paduka Ali, G. M. Hussey, *J. Org. Chem.* **2005**, *70*, 10875; c) H. Miyaji, W. Sato, J. L. Sessler, *Angew. Chem.* **2000**, *112*, 1847; *Angew. Chem. Int. Ed.* **2000**, *39*, 1777; d) H. Miyaji, J. L. Sessler, *Angew. Chem.* **2001**, *113*, 158; *Angew. Chem. Int. Ed.* **2001**, *40*, 154, and references cited therein.

[3] a) J. S. Kim, S. J. Lee, J. H. Jung, I. Hwang, N. J. Singh, S. K. Kim, S. H. Lee, H. J. Kim, C. S. Keum, J. W. Lee, K. S. Kim, *Chem. Eur. J.* **2007**, *13*, 3082; b) J. H. Jung, S. J. Lee, J. S. Kim, W. S. Lee, Y. Sakata, T. Kaneda, *Org. Lett.* **2006**, *8*, 3009; c) N. A. Rakow, A. Sen, M. C. Janzen, J. B. Ponder, K. S. Suslick, *Angew. Chem.* **2005**, *117*, 4604; *Angew. Chem. Int. Ed.* **2005**, *44*, 4528; d) Y. Imai, N. Tajima, T. Sato, R. Kuroda, *Org. Lett.* **2006**, *8*, 2941; e) Y. Imai, N. Tajima, T. Sato, R. Kuroda, *Chirality* **2002**, *14*, 604.

[4] Y.-P. Tseng, G.-M. Tu, C.-H. Lin, C.-T. Chang, C.-Y. Lin, Y.-P. Yen, *Org. Biomol. Chem.* **2007**, *5*, 3592.

[5] F. L. Dickert, P. Lieberzeit, M. Tortschanoff, *Sens. Actuators B* **2000**, *65*, 186.

[6] P. Sahoo, D. Krishna kumar, D. R. Trivedi, P. Dastidar, *Tetrahedron Lett.* **2008**, *49*, 3052.

[7] A. Babai, A. Mudring, *Inorg. Chem.* **2006**, *45*, 4874.

[8] K.-S. Huang, D. Britton, M. C. Etter, S. R. Byrn, *J. Mater. Chem.* **1997**, *7*, 713.

[9] a) A. V. Trask, W. Jones, *Top. Curr. Chem.* **2005**, *254*, 41, and references cited therein; b) F. Toda, *Acc. Chem. Res.* **1995**, *28*, 480.

[10] S. V. Bhosale, C. H. Jani, S. J. Langford, *Chem. Soc. Rev.* **2008**, *37*, 331.

[11] L. R. MacGillivray, J. L. Reid, J. A. Ripmeester, *J. Am. Chem. Soc.* **2000**, *122*, 7817.

[12] D. R. Trivedi, Y. Fujiki, Y. Goto, N. Fujita, S. Shinkai, K. Sada, *Chem. Lett.* **2008**, *37*, 550.

[13] J. Mizuguchi, T. Makino, Y. Imura, H. Takahashi, S. Suzuki, *Acta. Crystallogr. Sect. E* **2005**, *61*, o3044.